

# NAD(P)H-quinone oxidoreductase 1 induces complicated effects on mitochondrial dysfunction and ferroptosis in an expression level-dependent manner

Jaewang Lee<sup>#</sup>, Dong-Hoon Hyun<sup>\*</sup>

Department of Life Science, Ewha Womans University, Seoul, South Korea.

**SUMMARY** NAD(P)H-quinone oxidoreductase 1 (NQO1) is an essential redox enzyme responsible for redox balance and energy metabolism. Despite of its importance, the brain contains high capacity of polyunsaturated fatty acids and maintains low levels of NQO1 expression. In this study, we examined how levels of NQO1 expression affects cell survival in response to toxic insults causing mitochondrial dysfunction and ferroptosis, and whether NQO1 has a potential as a biomarker in different stressed conditions. Following treatment with rotenone, overexpressed NQO1 in SH-SY5Y cells improved cell survival by reducing mitochondrial reductive stress *via* increased NAD<sup>+</sup> supply without mitochondrial biogenesis. However, NQO1 overexpression boosted lipid peroxidation following treatment with RSL3 and erastin. A lipid droplet staining assay showed increased lipid droplets in cells overexpressing NQO1. In contrast, NQO1 knockdown protected cells against ferroptosis by increasing GPX4, xCT, and the GSH/GSSG system. Also, NQO1 knockdown showed lower iron contents and lipid droplets than non-transfectants and cells overexpressing NQO1, even though it could not attenuate cell death when exposed to rotenone. In summary, our study suggests that different NQO1 levels may have advantages and disadvantages depending on the surrounding environments. Thus, regulating NQO1 expression could be a potential supplementary tool when treating neuronal diseases.

**Keywords** NQO1, mitochondrial biogenesis, NAD<sup>+</sup>, lipid peroxidation, ferroptosis, reductive stress

## 1. Introduction

Energy metabolism is a vital process for cell survival. Cells generate adenosine triphosphate (ATP) mainly *via* mitochondrial respiration requiring carbon sources and electron donors. Primarily, cells break glucose and glutamine into small molecules, and provide with carbons and transfer electrons in forms of nicotinamide adenine dinucleotide (NADH) or flavin adenine dinucleotide (FADH<sub>2</sub>), resulting in ATP production in the mitochondria. In rapidly proliferating cells, energy demands are increased to meet growing cellular biomass. Nicotinamide adenine dinucleotide (NAD<sup>+</sup>) is an important electron carrier for activating energy metabolism, and converted to NADH by acquiring electrons during metabolic processes (1). NADH transfers electrons to biomolecules for their activation. NAD<sup>+</sup> is a coenzyme for the redox balance and activates non-redox NAD<sup>+</sup>-dependent enzymes such as sirtuins and poly(ADP-ribose) polymerase (PARP) (2). Furthermore, nicotinamide adenine dinucleotide phosphate (NADP<sup>+</sup>) plays a significant role in cell metabolism such as

oxidative stress (*e.g.*, the GSH/GSSG system) and anabolic pathways (*e.g.*, fatty acid synthesis). Low NAD(P)<sup>+</sup> levels are linked to many diseases including metabolic dysfunction and neurodegenerative diseases. Also, mitochondrial dysfunction promoted by metabolic stress exacerbates progressive oxidative damage, resulting in neurodegenerative diseases. A recent study showed that *de novo* NAD<sup>+</sup> synthesis fortified mitochondrial functions and improved health, suggesting that restoring NAD<sup>+</sup> levels is a potential therapeutic target for some diseases. These characteristics make NAD<sup>+</sup> central to energy metabolism.

NAD(P)H-quinone oxidoreductase 1 (NQO1) is a phase II antioxidant enzyme capable of detoxification and NAD<sup>+</sup> supply through two electron transfer without semiquinone radical production (3). Increased NQO1 could boost mitochondrial functions (4,5). By contrast, NQO1-mediated futile redox cycling of  $\beta$ -lapachone causes oxidative stress by damaging DNA, hyperactivating PARP, and depleting NAD<sup>+</sup> and ATP (6).  $\beta$ -Lapachone could decrease inositol pyrophosphates by NQO1 (7). These results suggest that understanding

two-sided effects of NQO1 is essential to regulate cellular environments properly. However, most studies for a disease therapy are focused on attenuating reactive oxygen species (ROS) levels by increasing NQO1 activity or expression levels.

Ferroptosis is a regulated cell death induced by iron-dependent lipid peroxidation (8). Ferroptosis can be caused by inhibiting glutathione peroxidase 4 (GPX4) or system xc<sup>-</sup> cystine/glutamate antiporter (xCT) (9). GPX4 oxidizes glutathione (GSH) and converts lipid peroxyl radicals to lipid alcohols. GPX4 inhibition cannot protect cells against lipid peroxidation following (1S,3R)-RSL3 (RSL3) treatment (10). xCT involved in GSH synthesis is another central ferroptosis regulator. Inhibited xCT depletes GSH synthesis in the presence of erastin. GSH deficiency hinders the redox cycle *via* GPX4, and ultimately promotes ferroptosis by decreasing neutralization of lipid peroxyl radicals (11). xCT inhibition also attenuates glutamine metabolism and lowers nutrient flexibility (12). Acyl-CoA synthetase long-chain family member 4 (ACSL4) increases levels of polyunsaturated fatty acids (PUFAs), raising sensitivity to ferroptosis by increasing lipid peroxidation (13). Moreover, high levels of lipid droplets could proportionally elevate susceptibility to ferroptosis because of elevated PUFAs and lipophagy activation (14). Meanwhile, epithelial-mesenchymal transition (EMT) shifted glucose-dependent metabolism to lipid-dependent metabolism and increased ferroptosis sensitivity (14,15). Increased cellular density in cancers reduced ferroptosis, but cells with mesenchymal traits had enhanced ferroptosis sensitivity (14,15). These reports indicate that differentiated or undifferentiated neuronal cells may have different responses to ferroptosis inducers, considering that their morphologies are different, similar to cells with epithelial or mesenchymal characteristics (16).

NQO1 as a NAD<sup>+</sup> supplier or an antioxidant is an important factor in attenuating cellular stress. Still, little has been studied on its adverse effects on neural cells. In this study, effects of NQO1 expression on different environments and its potential as biomarker were examined.

## 2. Materials and Methods

### 2.1. Cell culture and reagents

SH-SY5Y cells (ATCC, Manassas, VA, USA) were cultured in Dulbecco's Modified Eagle's Medium supplemented with 10% fetal bovine serum, 1% antibiotic-antimycotic including 100 IU/ml penicillin, 100 µg/ml streptomycin and 0.25 µg/ml amphotericin B in a humidified 5% CO<sub>2</sub>/95% air atmosphere. All materials required for cell culture were purchased from Thermo Fisher Scientific (Waltham, MA, USA). Cells were treated with rotenone (Sigma Aldrich, St. Louis,

MO, USA), (1S, 3R)-RSL3 (Cayman Chemical Co., Ann Arbor, MI, USA), or erastin (Selleckchem, Houston, TX, USA). The following is a diagram to show the protocol of the present study (Figure S1, <https://www.biosciencetrends.com/supplementaldata/196>).

### 2.2. Cell viability and death assays

Cell viability was assessed using the Cell Counting Kit-8 (CCK-8; Dojindo Laboratories, Tokyo, Japan), as described by the manufacturer's protocol. Cells (1x10<sup>4</sup> cell/well) were seeded in a 12-well culture plate. Cells at 70% confluency were pretreated with dicoumarol for 2 h, and then exposed to rotenone, RSL3, or erastin. The equivalent amount of dimethyl sulfoxide (DMSO) was used as controls. Cells were incubated with CCK-8 solution for 1 h at 37°C, and absorbance was measured at 450 nm using the SpectraMax M3 microplate reader (Molecular Devices, Sunnyvale, CA, USA). LDH assay was performed using the Cytotoxicity LDH Assay Kit-WST (Dojindo Laboratories), according to the manufacturer's protocol. After treatment for 24 h, the lysis buffer was added to samples, and incubated for 30 min at 37°C. The working solution was treated for 30 min at room temperature (RT), and then the stop solution was added to the mixtures. Absorbance was read at 490 nm. ATP-based cell viability was measured using CellTiter-Glo 2.0 (Promega, Pittsburg, WI, USA). After exposure to rotenone, N-acetyl-L cysteine (NAC; Sigma-Aldrich), or nicotinamide mononucleotide (NMN; Sigma-Aldrich) for 24 h at 37°C, cells were incubated with CellTiter-Glo 2.0 solution for 30 min at RT. Luminescence was measured using the SpectraMax M3 microplate reader. Cell death after rotenone treatment was examined using 5 µM SYTOX Green (Thermo Fisher Scientific). Stained cells were observed using the ECLIPSE Ts2R fluorescent microscope (Nikon, Tokyo, Japan). Dead cells were quantified by counting SYTOX Green-positive cells. For the colony formation assay, cells were seeded 500 cells/well into a 6-well plate. After 14 days in culture, cells were stained with a 0.5% crystal violet solution, and the number of colonies was counted.

### 2.3. Measurement of GSH, ROS production, lipid ROS, mitochondrial superoxide, and mitochondrial membrane potential

GSH levels were measured using the EnzyChrom GSG/GSSG Assay Kit (BioAssay System, Hayward, CA, USA), according to the manufacturer's procedure. ROS generation was assessed using 10 µM 2',7'-dichlorofluorescein diacetate (DCFDA; Abcam, Cambridge, UK) following culturing cells with or without rotenone for 8 h. Stained cells were incubated for 30 min at 37°C. Fluorescence was measured using the SpectraMax M3 microplate reader and the CytoFLEX

flow cytometer (Beckman Coulter, Chaska, MN, USA). Lipid ROS was determined by staining cells with 5  $\mu$ M BODIPY 581/591 C11 (Thermo Fisher Scientific, Waltham, MA, USA). After 30 min at 37°C, intensity was measured by the CytoFLEX flow cytometer. Mitochondrial superoxide was examined using 1  $\mu$ M MitoSOX (Thermo Fisher Scientific). After 30 min at 37°C, stained cells were analyzed by the CytoFLEX flow cytometer and ECLIPSE Ts2R fluorescent microscope at 612 nm. Images were quantified using the Image J software. Mitochondria membrane potentials were measured by staining cells with 200 nM tetramethyl rhodamine ethyl ester (Thermo Fisher Scientific) for 20 min. Fluorescence was measured every 2 h using the SpectraMax M3 microplate reader. Mean fluorescent intensity of each group was normalized to that of the control group for quantification.

#### 2.4. Iron measurements

Intracellular iron contents were also quantified using the Iron Assay Kit (Sigma-Aldrich) according to the manufacturer's guide. Intracellular ferrous iron was stained with FerroOrange (Dojindo Laboratories), and mitochondrial ferrous iron levels were assayed using 5  $\mu$ M Mito-FerroGreen (Dojindo Laboratories). Stained cells were observed by the ECLIPSE Ts2R fluorescent microscope at 546 nm and 455 nm, respectively. Images were quantified using the Image J software.

#### 2.5. RNA interference, transfection, gene overexpression and gene mutation

For NQO1 knockdown, cells were stably transfected with four short hairpin RNAs (shRNAs) targeting *NQO1* mRNA (pGPU6/Neo, GenePharma, Shanghai, China) using Lipofectamine 3000 reagent (Thermo Fisher Scientific). NQO1 expression levels were confirmed by immunoblot analysis, and the #4 construct was chosen (Table 1 and Figure S2D, <https://www.biosciencetrends.com/supplementaldata/196>). For NQO1 overexpression, pUCIDT(Amp)-NQO1 (Integrated DNA Technologies, Coralville, IA, USA) was digested by Hind III and Not I, and NQO1 fragment was inserted into pcDNA3.1(+) mammalian expression vector (Thermo Fisher Scientific). Cells were seeded and stably transfected with a control plasmid (Thermo Fisher Scientific) or pcDNA3.1-NQO1 plasmid using Lipofectamine 3000 reagent. For designing the mutant form, the mutation site was determined according to a previous report (17). The NQO1<sup>Y128F</sup> mutant construct was designed using EZchange Site-Directed Mutagenesis Kit (Enzynomics, Daejeon, South Korea) according to the manufacturer's procedure. The mutation was ordered and confirmed by DNA sequencing (Macrogen, Seoul, South Korea). NQO1 expression levels were confirmed by immunoblot analysis.

**Table 1. The sequences of RT-qPCR primers and shRNAs targeting *NQO1***

Name	Sequences
<i>MDH1</i>	F: 5'-CCAGGGTGCAGCCTTAGATA-3' R: 5'-TGAAGTTCTCCTTGGGGATG-3'
<i>MDH2</i>	F: 5'-GGTTTCCATCAGTGGCTAA-3' R: 5'-TTCAGAGGCCACAGTGTCTG-3'
<i>NQO1</i>	F: 5'-GTTGCCTGAAAAATGGGAGA-3' R: 5'-AAAAACCACAGTGCCAGTC-3'
<i>ACTB</i>	F: 5'-CTCTTCCAGCCTTCCTTCCT-3' R: 5'-AGCACTGTGTGGCGTACAG-3'
<i>LDHA</i>	F: 5'-TGGCAGCCTTTTCCTTAGAA-3' R: 5'-CTTTCTCCCTCTTGTCTGACG-3'
<i>LDHB</i>	F: 5'-TGTGAATGTGGCAGGTGTTT-3' R: 5'-GGCACTTCAACCACCATCT-3'
<i>GOT2</i>	F: 5'-GTCCTCCCATCTTGGAAACA-3' R: 5'-GCATTATTCCCTTGGGA-3'
<i>FH</i>	F: 5'-TGACAAGGCAGCAAAGATTG-3' R: 5'-ACCCATTCGTCAAACCTGCTC-3'
<i>SDHA</i>	F: 5'-GATTACTCCAAGCCCATCCA-3' R: 5'-GTTTTGTGCGATCACGGGTCT-3'
<i>SDHB</i>	F: 5'-CAATGAACATCAATGGAGGC-3' R: 5'-CTTGCCTTCTGAGATTCAT-3'
<i>OGDH</i>	F: 5'-ACTGGCTGCTCTGTCTTGGT-3' R: 5'-CCCTCTTCTGACCTGCTTTG-3'
<i>ACO2</i>	F: 5'-GAAATTGAGCGAGGCAAGTC-3' R: 5'-CAGATGGTCACAGTGGATGG-3'
<i>CPT1A</i>	F: 5'-TCGTCACCTTCTGCCTTT-3' R: 5'-GGGTCTGGCTTGTGATAA-3'
<i>GLS2</i>	F: 5'-GTGCACTGTGGATGGTCAAC-3' R: 5'-GTGCTAGGGTGTCTTATGGA-3'
shRNA sequences	
#1	S: 5'-CACCGGTTTGGAGCGAGTGTTCATAGTTCAAGA GACTATGAACACTCGCTCAAACCTTTTTTG-3' A: 5'-GATCCAAAAAAGGTTTGGAGCGAGTGTTCATA GTCTCTTGAACATGAACACTCGCTCAAACC-3'
#2	S: 5'-CACCGCAGACGCCGAATTCAAATCTTCAAGA GAGATTTGAATTCGGGCGTCTGCTTTTTTG-3' A: 5'-GATCCAAAAAAGCAGACGCCCGAATTCAAAT CTCTCTTGAAGATTGAAATTCGGGCGTCTGC-3'
#3	S: 5'-CACCGCAGCCTCTTGGACCTAAACTTTCAAGA GAAGTTTAGGTCAAAGAGGCTGCTTTTTTG-3' A: 5'-GATCCAAAAAAGCAGCCTCTTGGACCTAAACT TCTCTTGAAGTTTAGGTCAAAGAGGCTGC-3'
#4	S: 5'-CACCGGCCAATTCAGATGGCATTCTTCAAGA GAGAATGCCACTCTGAATTTGGCTTTTTTG-3' A: 5'-GATCCAAAAAAGGCCAATTCAGAGTGCATT CTCTCTTGAAGAATGCCACTCTGAATTTGCC-3'

#### 2.6. Reverse transcription-quantitative PCR and immunoblot analysis

When cells were 70% confluent, they were treated with indicated drugs. According to the manufacturer's instructions, total RNA from treated cells were extracted using QIAwave RNA Mini Kit (Qiagen, Venlo, Netherlands). Reverse transcription-quantitative polymerase chain reaction (RT-qPCR) was conducted using AccuPower 2X GreenStar™ qPCR Master Mix with 80X ROX (Bioneer, Daejeon, South Korea) after performing complementary DNA (cDNA) synthesis using AccuPower RT-PCR PreMix & Master Mix (Bioneer). *NQO1*, *LDHA*, *LDHB*, *CPT1A*, *MDH1*,

*MDH2*, *FH*, *SDHA*, *SDHB*, *OGDH*, *ACO2*, *GLS2*, *GOT2*, and *ACTB* (Table 1) were amplified. Relative target mRNA levels were determined using the  $2^{-\Delta\Delta Ct}$  method, and normalized against *ACTB* mRNA levels. mRNAs levels were confirmed by the StepOnePlus (Applied Biosystems, Foster City, CA, USA). For immunoblot analysis, cells were lysed using Cell Lysis Buffer (Cell Signaling Technology, Danvers, MA, USA) containing a protease/phosphatase inhibitor cocktail (Cell Signaling Technology). Cell lysates were resolved using 6%–15% SDS gels, separated proteins were transferred to nitrocellulose membranes, and then probed with appropriate primary and secondary antibodies. Following primary antibodies were used: NQO1, Nrf2 and Keap1 were purchased from GeneTex (Irvine, CA, USA); PGC-1 $\alpha$ , SIRT1, xCT, NDUFA9, SDHB, UQCRC2, COX IV, ATP5A, aconitase 2, MnSOD, FTH1, NCOA4 and GPX4 from Abcam (Cambridge, UK); SIRT3 and E-cadherin from Thermo Fisher Scientific; PARP from Cell Signaling; ACSL4 and vimentin from Santa Cruz Biotechnology (Dallas, TX, USA); and FPN and Tfr from Novus Biologicals (Littleton, CO, USA). Antibodies against  $\alpha$ -tubulin (GeneTex, Irvine, CA, USA) or  $\beta$ -actin (BioWorld, Atlanta, GA, USA) were served as total loading controls. All antibodies were diluted to concentrations between 1:500 and 1:30,000.

### 2.7. Measurement of NAD<sup>+</sup>/NADH ratio

When cells had grown to 70% confluency, NAD<sup>+</sup>/NADH ratio was measured using NAD<sup>+</sup>/NADH Assay Kit (Abcam), according to the manufacturer's instructions. NAD<sup>+</sup>/NADH ratio was determined by subtracting NADH from total NAD followed by dividing the product by NADH. Relative quantities of the NAD<sup>+</sup>/NADH ratio among groups were normalized against the control.

### 2.8. Measurement of malondialdehyde (MDA)

When cells had grown to 70% confluency, cells were treated with rotenone, RSL3, or erastin with indicated doses for 12 h. Cells were lysed to measure levels of lipid peroxidation using Malondialdehyde (MDA) Assay Kit (Abcam), according to the manufacturer's procedures.

### 2.9. Measurement of mitochondria complex I activity

When cells had grown to 90% confluency, mitochondrial fractions were isolated using Mitochondria Isolation Kit for Cultured Cells (Abcam). The mitochondria complex I activity was measured using the Mitochondrial Complex I activity Assay Kit (Sigma Aldrich), according to the manufacturer's procedures.

### 2.10. Staining of the mitochondria and lipid droplets

Cells were stained with 5  $\mu$ M MitoTracker Red CMXRos (Thermo Fisher Scientific) to confirm mitochondrial change and obtained images were quantified using Image J software. Cells were stained with BODIPY 493/503 (Thermo Fisher Scientific) to observe lipid droplets, and lipid droplets were counted for quantification.

### 2.11. Statistical analysis

Data were presented as average  $\pm$  standard error of means (SEM) after Kolmogorov-Smirnov test. Statistically significant differences between treatment groups were assessed using the Mann-Whitney *U*-test or analysis of variance (ANOVA) with the Bonferroni post-hoc test. All statistical tests were two-sided, and a *P* value of < 0.05 was statistically significant. The statistical tests were performed using IBM SPSS Statistics version 22.0 (IBM, Armonk, NY, USA).

## 3. Results

### 3.1. NQO1 overexpression does not change cellular ROS levels and expression of metabolic enzymes

NQO1 plays a significant role in cell survival by providing NAD(P)<sup>+</sup> and maintenance of redox homeostasis (Figure 1A), but SH-SY5Y cells tend to express low NQO1 levels (18). NQO1 was stably

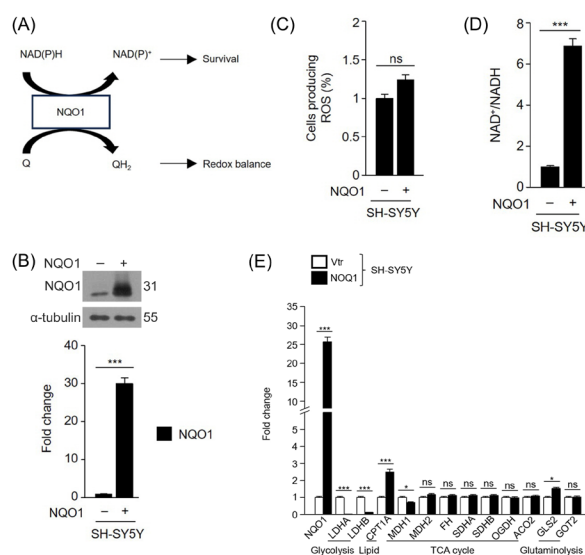


**Figure 1. NQO1 overexpression increases NAD<sup>+</sup> but decreases basal ROS levels.** (A) A schematic image of NQO1 functions. (B) Expression levels of NQO1 mRNA in SH-SY5Y with or without NQO1 transfection were confirmed using RT-qPCR and immunoblot analysis. (C) NAD<sup>+</sup>/NADH ratio was measured by NAD<sup>+</sup>/NADH assay in SH-SY5Y in the presence or absence of NQO1 transfection. (D) Cellular basal ROS levels were measured vis FACS using DCFDA for 20 min and then quantified. (E) Basal mRNA levels of metabolic proteins in vector control and NQO1 transfectant were examined using RT-qPCR. The results were normalized to vector control. Values are average  $\pm$  SEM from three independent experiments. ns, not significant. \**P* < 0.05, \*\*\**P* < 0.001 relative to their parental cells.

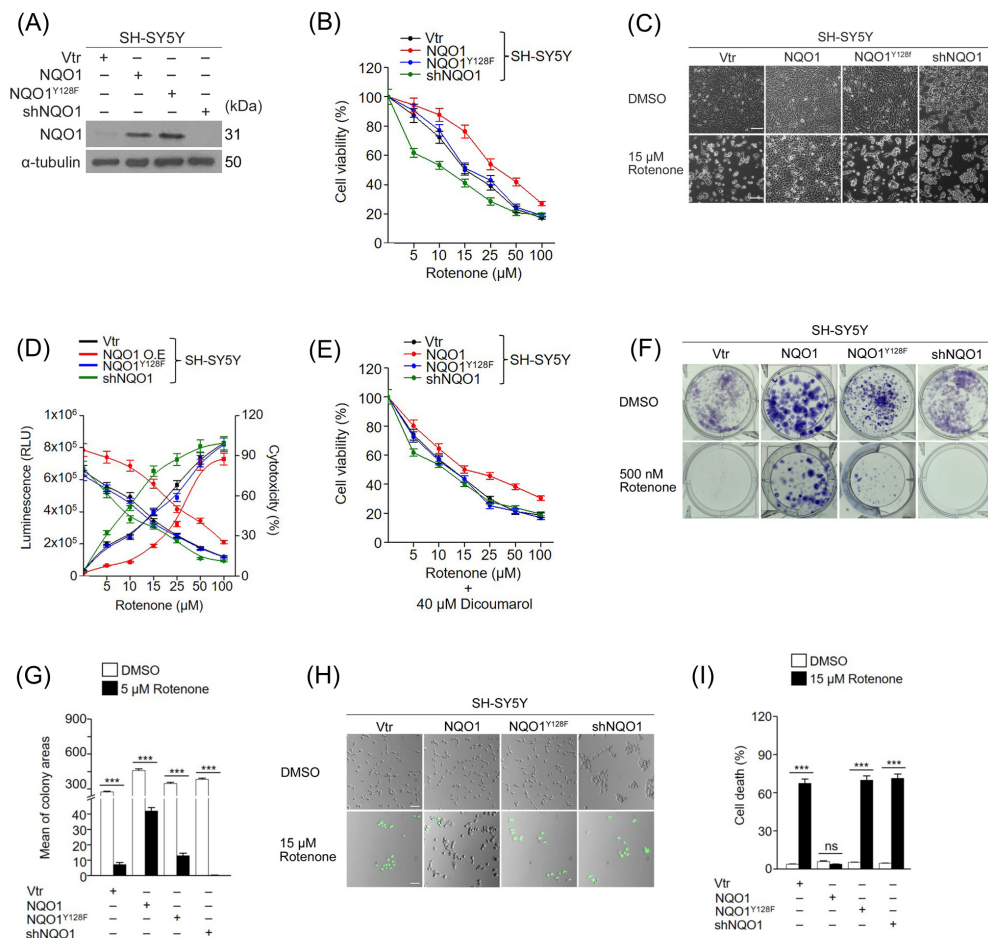


**Figure 2. NQO1 protects cells from toxic insults.** (A) NQO1 overexpression, NQO1<sup>Y128F</sup> mutant form, and NQO1 knockdown were confirmed by immunoblot analysis. (B) Cell viability was measured following exposure to rotenone with indicated doses for 24 h. (C) Cell morphological images were captured by a bright-field microscope after addition of 15  $\mu$ M rotenone. Original magnification, x100. Scale bar size, 100  $\mu$ m. (D) ATP-based cell viability assay was measured by CellTiter-Glo. Cytotoxicity was measured by LDH assay. (E) Cell viability change was determined after rotenone addition to cells pretreated with 40  $\mu$ M dicoumarol. (F, G) The clonogenic assay using 0.5% crystal violet was assessed after cells cultured with or without 5  $\mu$ M rotenone. Colony areas were quantified using the Image J software. (H, I) Cell death was assessed using 5  $\mu$ M SYTOX green following treatment of cells with 15  $\mu$ M rotenone for 24 h. Stained cells show dead cells. Stained images were quantified using the Image J software. Original magnification, x100. Scale bar size, 100  $\mu$ m. Data are average  $\pm$  SEM from three independent experiments. ns; not significant. \*\*\* $P < 0.001$  relative to DMSO treatment.

overexpressed (Figure 1B). NAD<sup>+</sup>/NADH ratio in cells overexpressing NQO1 was increased compared with that in non-transfectants ( $P < 0.001$ ) (Figure 1C). Total ROS levels were increased in cells transfected with NQO1 compared with those in control cells (Figure 1D). RT-qPCR results showed that levels of *LDHA* and *LDHB* were decreased, but *GLS2* (a glutaminolysis-related protein) and *CPT1A* (a fatty acid oxidation-related protein) increased in cells with high NQO1 levels. However, levels of cycle-related proteins were not significantly changed ( $P < 0.05$ , Figure 1E).

### 3.2. NQO1 protects SH-SY5Y cells against rotenone

Cells transfected with NQO1<sup>Y128F</sup> or shNQO1 were designed to compare cell survival under conditions of interference with energy metabolism (Figure 2A). Cell viability results showed that NQO1 overexpression rendered cells more resistant to rotenone than control

cells (Figure 2B-D). Pretreatment with dicoumarol greatly affected viability of NQO1-overexpressing cells after exposure to rotenone (Figure 2E). To confirm long-term effects of low doses of rotenone on cells, the colony formation test was performed. Colony formation results showed that NQO1 overexpression made cells less susceptible to rotenone than controls ( $P < 0.001$ , Figure 2F-G). In parallel, cell death was significantly attenuated in NQO1-overexpressing cells when exposed to rotenone, compared with others ( $P < 0.001$ , Figure 2H-I).

### 3.3. NQO1 inhibition increases GSH/GSSG dependency

Because oxidative stress is caused when the mitochondria complex I is inhibited by rotenone (19), ROS levels were measured by DCFDA staining, total GSH and GSH levels were assessed. NQO1-knockdown cells showed higher DCFDA staining. On the contrary, NQO1-

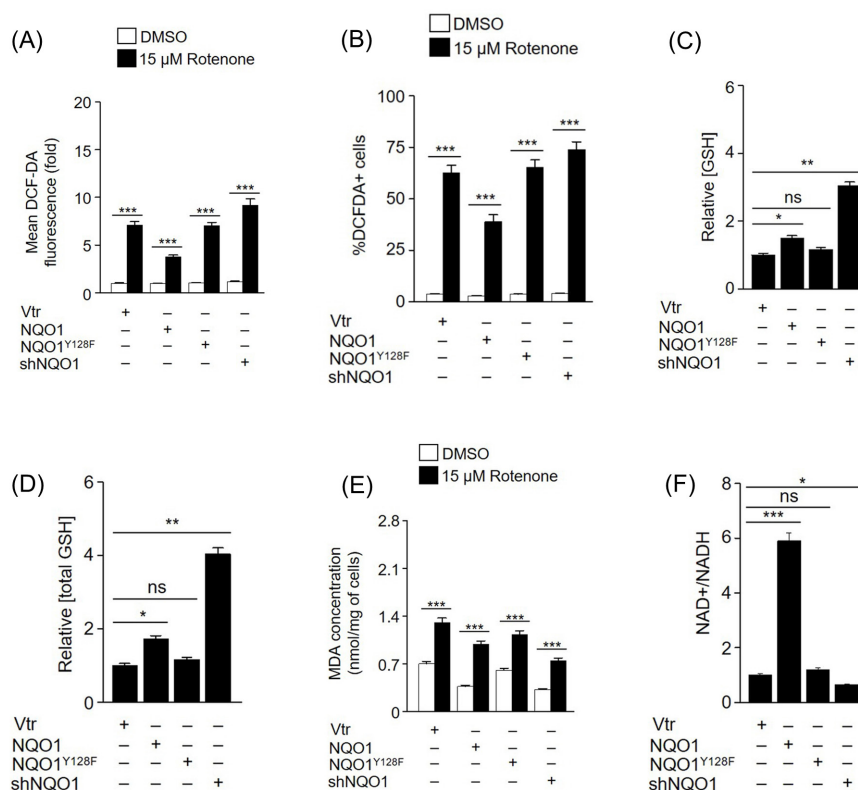


**Figure 3. NQO1 knockdown increases GSG/GSSG dependency.** (A, B) Cellular ROS levels were measured after cells were treated with 15 μM rotenone for 8 h and then were stained in 5 μM DCF-DA for 30 min. (C, D) GSH and total GSH levels under normal conditions were determined. (E) Cellular MDA contents were measured to determine lipid peroxidation after addition of 15 μM rotenone. (F) NAD<sup>+</sup>/NADH ratio was measured by the NAD<sup>+</sup>/NADH assay with no treatment. Values are average ± SEM from three independent experiments. ns; not significant; \**P* < 0.05, \*\**P* < 0.01, \*\*\**P* < 0.001 relative to DMSO treatment or vector control.

overexpressing cells showed lower DCFDA staining (*P* < 0.01, Figure 3A-B). There was no significant difference among control, NQO1<sup>Y128F</sup>, and NQO1 knockdown. Interestingly, both GSH levels were higher in NQO1-knockdown cells (*P* < 0.05, Figure 3C-D). Also, NQO1-knockdown cells showed lower MDA concentration when rotenone was added (*P* < 0.001, Figure 3E). NQO1 overexpression induced higher NAD<sup>+</sup>/NADH ratio, but NQO1 knockdown lower (*P* < 0.05, Figure 3F).

### 3.4. NQO1 overexpression does not boost mitochondrial biogenesis but decreases reductive stress by supplying NAD<sup>+</sup>

In order to confirm which of NQO1 functions (a NAD<sup>+</sup> provider and an antioxidant) is important for cell survival under conditions of rotenone treatment, ATP-based cell viability was performed using NAC (an antioxidant) and NMN (a NAD<sup>+</sup> precursor), respectively. Cell viability was higher in NMN-treated groups than in NAC-treated ones. Cell viability results implied that ATP production was higher after NMN addition compared to NAC treatment (*P* < 0.05, Figure 4A). This difference would be due to NAD<sup>+</sup> supply (*P* < 0.05, Figure 4B). The GSH-GSSG system can protect cells from ROS but cannot directly boost or maintain mitochondrial activity in the

presence of rotenone (*P* < 0.05, Figure 4C).

Considering previous studies showed that increasing NQO1 could increase mitochondrial activity (20) and NAD<sup>+</sup> produced by NQO1 could promote mitochondrial biogenesis by activating the PGC-1α-SIRT1 axis (21), the extent of mitochondrial biogenesis in cells with control, NQO1 overexpression, NQO1<sup>Y128F</sup>, or shNQO1 were determined. Immunoblot results showed that levels of PGC-1α were increased in NQO1-overexpressing cells compared with others. Likewise, PGC-1α levels were decreased in NQO1 knockdown cells. SIRT3 (a critical molecule involved in mitochondrial biogenesis) levels were not significantly changed among all groups. SIRT1 was higher in NQO1 knockdown cells. PARP (a NAD<sup>+</sup>-consuming protein) levels were also dramatically elevated in both NQO1-overexpressing cells and NQO1-knockdown cells. Immunoblot analysis for confirming oxidative stress showed that Nrf2 levels were increased and Keap1 levels were decreased slightly in NQO1-overexpressing cells and NQO1-knockdown cells. Levels of all NAD<sup>+</sup>-consuming proteins were increased in both NQO1-overexpressing cells and NQO1-knockdown cells (Figure 4D).

Levels of ETC proteins among all groups were measured to observe whether expression levels of mitochondrial proteins involved in oxidative

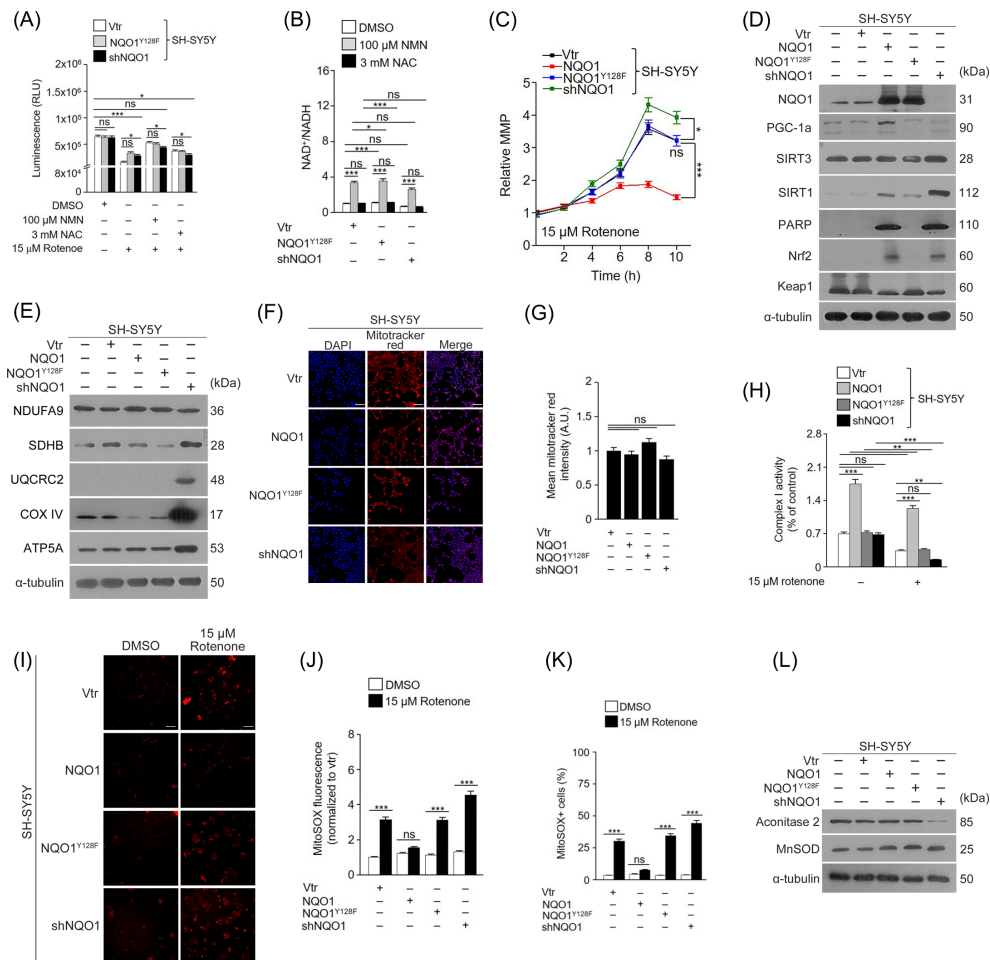


**Figure 4. Biogenesis is not the main factor of cell survival under conditions of complex I inhibition.** (A) ATP levels were indirectly measured using CellTiter-Glo after cells were subjected to 15 μM rotenone, 100 μM NMN, and 3 mM NAC for 24 h. (B) NAD<sup>+</sup>/NADH ratio was measured after treatment with 15 μM rotenone, 200 μM NAM, and 3 mM NAC for 24 h. (C) Mitochondrial activity was determined using MMP following exposure of cells to 15 μM rotenone. (D, E) Levels of proteins responsible for mitochondrial biogenesis were assessed by immunoblot analysis. (F, G) The mitochondria were visualized by staining cell with 5 μM MitoTracker Red for 20 min, and their fluorescent images were quantified using the Image J software. Original magnification, x 200. Scale bar size, 50 μm. (H) The complex I activity was measured after being treated with 15 μM rotenone for 24 h to examine mitochondrial complex I efficiency. (I, K) Mitochondrial superoxide production was measured by FACS using 1 μM MitoSOX for 30 min after 15 μM rotenone treatment for 8 h. Intensity was quantified using the Image J software. Original magnification, x200. Scale bar size, 50 μm. (L) Mitochondrial stress was determined by immunoblot analysis. Data are average ± SEM from three independent experiments. ns; not significant. \**P* < 0.05, \*\**P* < 0.01, \*\*\**P* < 0.001 relative to DMSO treatment or vector control group.

phosphorylation were changed. NDUFA9 levels were slightly increased in cells overexpressing NQO1 compared with control cells. Levels of SDHB, UQCRC2, and ATP5A in NQO1-overexpressing cells were not significantly changed compared with control cells (Figure 4E and Figure S3A, <https://www.biosciencetrends.com/supplementaldata/196>). In contrast, levels of SDHB, UQCRC2, and ATP5A were significantly increased in NQO1-knockdown cells compared with others. NQO1 downregulation tended to decrease NDUFA9 levels. In particular, COX IV levels were greatly increased by NQO1 knockdown, but decreased by NQO1 overexpression (Figure 4E). Meanwhile, LDHA mRNA levels were increased in cells overexpressing NQO1 (Figure S3D, <https://www.biosciencetrends.com/supplementaldata/196>).

Examination of mitochondrial iron (a gist molecule

of the iron-sulfur cluster) contents showed that Mito-FerroGreen fluorescence intensity was not significantly changed between control cells and NQO1-overexpressing cells. However, Mito-FerroGreen fluorescence intensity was decreased in NQO1-knockdown cells (*P* < 0.01, Figure S3B-C, <https://www.biosciencetrends.com/supplementaldata/196>). Furthermore, MitoTracker staining images indirectly showed that the number of mitochondria was not significantly different among all groups (Figure 4F-G). On the contrary, NQO1-overexpressing cells maintained high complex I activity compared with other groups (*P* < 0.01, Figure 4H).

MitoSOX results indicated that mitochondrial ROS levels were lowered by NQO1 overexpression, but raised by NQO1 knockdown after exposure to rotenone (*P* < 0.05) (Figure 4I-K). Immunoblot analysis showed that

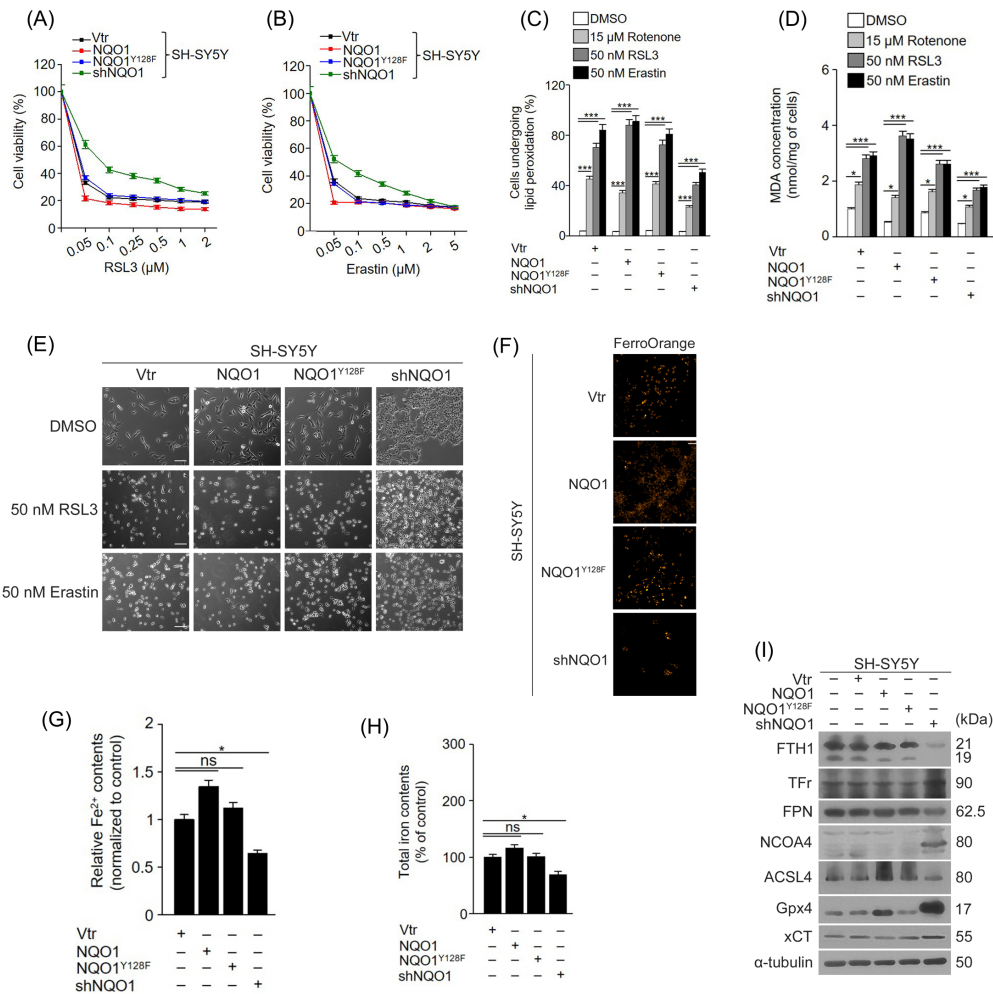


**Figure 5. NQO1 knockdown reduces sensitivity to ferroptosis.** (A, B) Cell viability change was assessed following treatment with RSL3 and erastin with indicated doses for 24 h. (C) Levels of lipid peroxyl were measured via FACS after cells were treated with 15 μM rotenone, 50 nM RSL3, and 50 nM erastin for 8 h and then stained with 5 μM BODIPY C-11 for 30 min. (D) Cellular MDA contents were measured following addition of 15 μM rotenone, 50 nM RSL3, or 50 nM erastin. (E) Bright-field microscope images after 50 nM RSL3 or 50 nM erastin treatment. Original magnification, x200. Scale bar size, 50 μm. (F, G) Cells were stained with 5 μM FerroOrange dye for 20 min to visualize relative ferrous iron levels, and fluorescent images were quantified by Image J software. Original magnification, x100. Scale bar size, 100 μm. (H) Cellular total iron contents were measured. (I) Expression of ferroptosis-related proteins under normal conditions was determined by immunoblot analysis were performed. Values are average ± SEM from three independent experiments. ns; not significant. \**P* < 0.05, \*\**P* < 0.01, \*\*\**P* < 0.001 relative to DMSO treatment or vector control.

under normal culture conditions, aconitase 2 levels were decreased and MnSOD levels were increased in NQO1 knockdown. However, aconitase 2 levels were not changed, and MnSOD2 levels were increased by NQO1 overexpression.

### 3.5. NQO1 knockdown endows cells with resistance to ferroptosis

When treated with RSL3 or erastin, a GPX4 inhibitor and an xCT inhibitor, respectively, cell viability was the highest in NQO1-knockdown cells at all indicated doses (except for 5 μM erastin) compared with others (Figure 5A-B). In addition, levels of lipid ROS (*P* < 0.001) and MDA (*P* < 0.05) were lower in cells with downregulated NQO1 (Figure 5C-D). Bright-field images showed

responses to ferroptosis inducers (Figure 5E). Levels of ferrous iron (Fe<sup>2+</sup>) and total iron were lower in NQO1-knockdown cells compared with others (*P* < 0.05, Figure 5F-H). Immunoblot analysis related to ferroptosis showed that expression levels of FTH1, ACSL4, and FPN were decreased in NQO1-knockdown cells compared with others (Figure 5I). However, Tfr, NCOA4, GPX4, and xCT levels were higher in cells with downregulated NQO1 than others. Moreover, NQO1-knockdown cells included a smaller number of lipid droplets compared with others (*P* < 0.01, Figure S4A-B, <https://www.biosciencetrends.com/supplementaldata/196>).

## 4. Discussion

Mitochondrial dysfunction is found at the early stage in

many neurodegenerative diseases. Under undesirable environments, cells can survive through metabolic shift and a compensatory mechanism such as activation of plasma membrane (PM) redox enzymes. Previous studies revealed that upregulated PM redox enzymes (e.g., NQO1, cytochrome b5 reductase) promoted mitochondrial functions under conditions of metabolic and proteotoxic stresses (22). These results emphasize the importance of PM redox enzymes in response to various toxic conditions. However, previous studies were focused on boosting NQO1 without considering whether low NQO1 levels benefit cells or what are benefits NQO1 offers to cells despite its low expression in neuronal cells.

This study demonstrated that SH-SY5Y cells could respond differently to toxic insults depending on NQO1 levels (Figure S1, <https://www.biosciencetrends.com/supplementaldata/196>). As described at the previous study (20), increased NQO1 reduced susceptibility to inhibition of the mitochondrial complex I. Although the GSH/GSSG system was significantly increased in NQO1-knockdown cells, ROS levels were still higher in NQO1-knockdown cells following rotenone treatment, compared with others (Figure 3A-B). This means that an antioxidant function of NQO1 might not be the most crucial factor for survival under complex I inhibition. This result suggests to consider another function of NQO1 as a key factor for cell survival in response to complex I inhibition. In addition, dramatic decreased levels of cellular ROS were not observed in cells overexpressing NQO1. Instead, cellular ROS levels were increased in both NQO1-overexpressing cells and NQO1-knockdown cells compared to those in control cells, even though there was no significant difference between them, possibly due to mild cellular stress. Assessment of GSH levels and immunoblot analysis using antibodies against Nrf2 and Keap1 supported that mild oxidative stress was continuous in both NQO1-overexpressing cells and NQO1-knockdown cells (Figure 3C and Figure 4D). Considering that  $\text{NAD}^+$  is a primary energy carrier in the mitochondria and NQO1 functions as an  $\text{NAD}^+$  provider, increased cellular ROS is likely due to elevated electron transport in the mitochondria through increased  $\text{NAD}^+$  levels in NQO1-overexpressing cells and due to reductive stress generated from decreased  $\text{NAD}^+/\text{NADH}$  ratio in NQO1-knockdown cells (Figure 3F) (23). It may be unusual that decreased NQO1 reduced  $\text{NAD}^+/\text{NADH}$  because high GSH contents mean increased  $\text{NAD(P)}^+$  levels (24), but it can be assumed that an available and absolute amount of  $\text{NAD}^+$  for the mitochondria may be diminished to maintain the GSH/GSSG cycle against increased ROS levels. Interestingly, highly increased NQO1 levels did not change expression levels of central metabolic proteins in the mitochondria. Instead, levels of glycolysis-related proteins were decreased and those of lipid metabolism-related proteins were increased. A meta-analysis of

human metabolism showed that  $\text{NAD}^+$  precursor supplementation activated lipid metabolism (25). This metabolic change seemed to be an action to prevent cell death and store energy sources because excessive ATP can induce apoptosis (26), consistent with increased levels of proteins responsible for lipid metabolism and lipid droplets (Figure 1E and Figure S4A-B, <https://www.biosciencetrends.com/supplementaldata/196>). By contrast, NQO1-knockdown cells exhibited increased aerobic glycolysis because increased demand for  $\text{NAD}^+$  can promote aerobic glycolysis and decrease proliferation (27). Moreover, NQO1-knockdown cells showed morphological alterations, similar to epithelial cells or undifferentiated forms. NQO1 knockdown induced decreased proliferation rate compared with others, and ATP production was decreased as if dormant. These results are consistent with a previous study.

Meanwhile, NQO1 knockdown made cells more sensitive to complex I inhibition because of declined  $\text{NAD}^+$  supply, but ROS levels were not significantly changed compared with control and NQO1<sup>Y128F</sup> cells. NQO1 knockdown boosted the GSH/GSSG system to compensate for NQO1 deficiency. Intriguingly, NQO1-knockdown cells showed lower MDA production compared with others, meaning that NQO1 knockdown reduced lipid peroxidation. Because cellular ROS can increase lipid peroxidation and MDA is a final product of lipid peroxidation (28), this result suggests that NQO1 knockdown in neuronal cells might be beneficial in response to ferroptosis. Thus, resistance to ferroptosis was compared among control, NQO1 overexpression, NQO1<sup>Y128F</sup>, and NQO1-knockdown cells. The result showed that NQO1 downregulation attenuated ferroptosis compared with other cells. Interestingly, NQO1-knockdown cells contained lower levels of iron and lipid droplets than other cells. Levels of FTH1 and FPN were decreased, but those of Tfr and NCOA4 increased by NQO1 downregulation. Decreased FTH1 and FPN and increased Tfr indicate that cells were exposed to iron deficiency (29). Increased NCOA4 showed that cells tried to store iron because decreased NCOA4 activated ferritinophagy to increase cellular iron levels (30). Immunoblotting results indicate that NQO1-knockdown cells were undergoing iron starvation responses. Although the exact reason was not assessed, decreased iron content is likely linked to reduced proliferation because proliferation requires more iron to make iron-sulfur clusters for producing new enzymes (31,32). Increased proliferation of cells overexpressing NQO1 is because of c-fos stabilization by NQO1 (33). Thus, decreased proliferation of NQO1-knockdown cells might result from the degradation of c-fos (33). Also, increased GPX4 and xCT and decreased ACSL4 in NQO1-knockdown cells would be the key factor in reducing ferroptosis when treated with RSL3 and erastin (34). Especially, decreased ACSL4 would explain why NQO1-knockdown cells preferred settlement to moving

because PUFAs are associated with increased membrane fluidity (35), and necessary for cellular migration because of their low rigidity (14,36). Moreover, morphological changes and expression levels of EMT-related molecules support that their different responses to ferroptosis are resulted from changes in cell characteristics because decreased e-cadherin can increase ferroptosis sensitivity (Figure S2A-D, <https://www.biosciencetrends.com/supplementaldata/196>) (15). In NQO1-knockdown cells, increased e-cadherin induced a partial EMT-like state, endowing cells with more resistance to ferroptosis than cells with low e-cadherin. Maintenance of the antioxidant system is especially important in neurons because of their low capacity of antioxidants (18). In this regard, high expression levels of xCT and GPX4 might help to boost the GSH/GSSG system in NQO1-knockdown cells to protect cells from ROS. Considering that many neurodegenerative diseases are related to oxidative stress generated by iron-dependent metabolic dysfunction (37), changes in the antioxidant system might be an evolutionary legacy to avoid ferroptosis. In contrast, NQO1 overexpression made cells susceptible to ferroptosis. Increased NQO1 decreased xCT levels because NQO1 can inhibit xCT *via* interacting with p53 (38). Increased sensitivity to ferroptosis in NQO1-overexpressing cells is resulted from increased content of iron and lipid droplets. However, iron levels in NQO1-overexpressing cells showed no significant difference compared to those of control cells, meaning that increased sensitivity to ferroptosis is caused by high PUFA contents, consistent with elevated ACSL4 (34). Increased PUFAs can promote lipid peroxidation, especially when ferroptosis inducers are existed. Although GPX4 levels were increased in NQO1-overexpressing cells compared with those of control cells, elevated lipid droplets and iron content might promote ferroptosis, causing lipid peroxidation to exceed the cellular capacity of dealing with ROS regardless of NQO1 and GPX4. Even decreased xCT levels would lower GPX4 synthesis (39).

Initially, it can be assumed that when NQO1 is overexpressed, mitochondrial biogenesis would be the main factor in cell survival under conditions of mitochondrial complex I inhibition because  $\text{NAD}^+$  stimulates the SIRT1-PGC-1 $\alpha$  axis (a critical factor for mitochondrial biogenesis) (40). However, evidence for mitochondrial biogenesis despite overexpressing NQO1 could not be found. Given that mitochondrial complex I inhibition can induce reductive stress (41), cellular protective effects would be because increased NQO1 supplies more  $\text{NAD}^+$  and blocks reductive stress induced by mitochondrial complex I inhibition, but not induced by mitochondrial biogenesis. Meanwhile,  $\text{NAD}^+$  was mostly consumed by PARP because the affinity of PARP to  $\text{NAD}^+$  is higher than that of NQO1 (42), meaning that PARP suppression is necessary to increase mitochondrial biogenesis. This phenomenon would be an action to

reduce energetic stress responses because increased  $\text{NAD}^+$  can cause energy deficiency (43). Although the exact reason why cells evolutionarily allow PARP to exhaust more  $\text{NAD}^+$  than SIRT1 is not known, it can be guessed that mostly exhausting  $\text{NAD}^+$  by PARP might help them to be ready to repair DNA damage and to inhibit excessive biogenesis due to a limited cellular capacity. Surprisingly, NQO1 knockdown also increased SIRT1 and PARP expression. Considering that levels of lactate and LDHA were increased (Figure 2D and Figure S3D, <https://www.biosciencetrends.com/supplementaldata/196>) in NQO1-knockdown cells, this might be due to the enhanced feedback for ATP demand and cellular stress from increasing lactate. Deficient ATP activates the AMPK-SIRT1 axis (44), and high lactate levels increase PARP expression (45). In addition, unexpectedly, levels of ETC proteins were increased in cells with downregulated NQO1 compared with NQO1-overexpressing cells. Since PGC-1 $\alpha$  was not changed but SIRT3 increased, this response might occur due to shortage of  $\text{NAD}^+$  supply. Because neurons lack metabolic plasticity (46) and increased glycolytic rate or glycogen synthesis can cause apoptosis (47), increased ETC proteins in NQO1-knockdown cells may be rebound responses to offset effects of decreased  $\text{NAD}^+$  supply and replenished ATP. Moreover, increased *LDHA* mRNA and GSH might help cells recycle  $\text{NAD}^+$  for respiration. Mitochondrial superoxide levels were lower under conditions of complex I inhibition, which supports that reductive stress was not increased in NQO1-overexpressing cells compared with others.

Taken together, cellular NQO1 levels have pros and cons. Many studies mainly focused on beneficial effects of increased NQO1 because of lower NQO1 expression in neurons. In addition, increased NQO1 protects cells from mitochondrial dysfunction. However, our results show that both NQO1 overexpression and NQO1 knockdown have advantages and disadvantages. NQO1 overexpression is advantageous to maintaining mitochondria-related functions when complex I is inhibited, but disadvantageous when exposed to ferroptosis inducers. NQO1 knockdown showed the opposite results against NQO1 overexpression. NQO1 knockdown has merits of inhibiting ferroptosis, although it has demerits of mitochondrial dysfunction. This means that different approaches should be used to treat neurodegenerative diseases in an NQO1 level-dependent manner.

There are several limitations to this study. Firstly, why increasing NQO1 led to accumulating lipid droplets could not be elucidated. Secondly, further experiments for lipid metabolites and lipid metabolism should be performed. Thirdly, whether changing different  $\text{NAD}^+$ -generating proteins produces same results needs to be assessed. Nonetheless, our study is worthwhile in noting that NQO1 can be a potentially useful target in an environment-dependent manner.

In conclusion, this study suggests that NQO1 levels can lead to different responses to complex I inhibition or ferroptosis inducers in neural cells. These might be a potential biomarker to choose an appropriate therapy. Increasing NQO1 may help alleviate Alzheimer's disease (AD) by reducing mitochondrial stress by amyloid  $\beta$ . In contrast, decreasing NQO1 may reduce a risk of  $\alpha$ -synuclein aggregation in Parkinson's disease (PD) by reducing hydroxy-2,3-trans-nonenal (4-HNE), potential to  $\alpha$ -synuclein aggregation. If combination therapy with NQO1 induction is considered, using ferroptosis inducers should be reconsidered. However, increasing NQO1 would be an effective approach to treat mitochondrial-related diseases induced by complex I dysfunction without ferroptosis induction. Since therapeutic studies using ferroptosis for cancer therapy and neurodegenerative diseases therapy have recently increased, regulating NQO1 would suggest a promising strategy for choosing an effective therapy.

### Acknowledgements

We thank Jihyun You at Seoul National University for providing us with ferroptosis and mitochondria activity-related materials.

**Funding:** This work was supported by the National Research Foundation of Korea (NRF) of the Korean Government (Grant No. NRF-2021R1F1A1051212) and by LogSynk (2-2021-1435-001).

**Conflict of Interest:** The authors have no conflicts of interest to disclose.

### References

- Spinelli JB, Haigis MC. The multifaceted contributions of mitochondria to cellular metabolism. *Nat Cell Biol.* 2018; 20:745-754.
- Covarrubias AJ, Perrone R, Grozio A, Verdin E. NAD<sup>+</sup> metabolism and its roles in cellular processes during ageing. *Nat Rev Mol Cell Biol.* 2021; 22:119-141.
- Monks TJ, Hanzlik RP, Cohen GM, Ross D, Graham DG. Quinone chemistry and toxicity. *Toxicol Appl Pharmacol.* 1992; 112:2-16.
- Hyun DH, Emerson SS, Jo DG, Mattson MP, de Cabo R. Calorie restriction up-regulates the plasma membrane redox system in brain cells and suppresses oxidative stress during aging. *Proc Natl Acad Sci U S A.* 2006; 103:19908-19912.
- Kim J, Kim SK, Kim HK, Mattson MP, Hyun DH. Mitochondrial function in human neuroblastoma cells is up-regulated and protected by NQO1, a plasma membrane redox enzyme. *PLoS One.* 2013; 8:e69030.
- Bey EA, Reinicke KE, Srougi MC, *et al.* Catalase abrogates beta-lapachone-induced PARP1 hyperactivation-directed programmed necrosis in NQO1-positive breast cancers. *Mol Cancer Ther.* 2013; 12:2110-2120.
- Eisenbeis VB, Qiu D, Gorka O, Strotmann L, Liu G, Prucker I, Su XB, Wilson MSC, Ritter K, Loenarz C, Gross O, Saiardi A, Jessen HJ. beta-lapachone regulates mammalian inositol pyrophosphate levels in an NQO1- and oxygen-dependent manner. *Proc Natl Acad Sci U S A.* 2023; 120:e2306868120.
- Stockwell BR, Friedmann Angeli JP, Bayir H, *et al.* Ferroptosis: A regulated cell death nexus linking metabolism. *Redox Biology and Disease. Cell.* 2017; 171:273-285.
- Angeli JPF, Shah R, Pratt DA, Conrad M. Ferroptosis inhibition: mechanisms and opportunities. *Trends Pharmacol Sci.* 2017; 38:489-498.
- Hangauer MJ, Viswanathan VS, Ryan MJ, Bole D, Eaton JK, Matov A, Galeas J, Dhruv HD, Berens ME, Schreiber SL, McCormick F, McManus MT. Drug-tolerant persister cancer cells are vulnerable to GPX4 inhibition. *Nature.* 2017; 551:247-250.
- Liu L, Liu R, Liu Y, Li G, Chen Q, Liu X, Ma S. Cystine-glutamate antiporter xCT as a therapeutic target for cancer. *Cell Biochem Funct.* 2021; 39:174-179.
- Shin CS, Mishra P, Watrous JD, Carelli V, D'Aurelio M, Jain M, Chan DC. The glutamate/cystine xCT antiporter antagonizes glutamine metabolism and reduces nutrient flexibility. *Nat Commun.* 2017; 8:15074.
- Jia B, Li J, Song Y, Luo C. ACSL4-mediated ferroptosis and its potential role in central nervous system diseases and injuries. *Int J Mol Sci.* 2023; 24:10021.511.
- You JH, Lee J, Roh JL. PGRMC1-dependent lipophagy promotes ferroptosis in paclitaxel-tolerant persister cancer cells. *J Exp Clin Cancer Res.* 2021; 40:350.
- Lee J, You JH, Kim MS, Roh JL. Epigenetic reprogramming of epithelial-mesenchymal transition promotes ferroptosis of head and neck cancer. *Redox Biol.* 2020; 37:101697.
- Kovalevich J, Langford D. Considerations for the use of SH-SY5Y neuroblastoma cells in neurobiology. *Methods Mol Biol.* 2013; 1078:9-21.
- Ma Q, Cui K, Xiao F, Lu AY, Yang CS. Identification of a glycine-rich sequence as an NAD(P)H-binding site and tyrosine 128 as a dicumarol-binding site in rat liver NAD(P)H:quinone oxidoreductase by site-directed mutagenesis. *J Biol Chem.* 1992; 267:22298-22304.
- Ahlgren-Beckendorf JA, Reising AM, Schander MA, Herdler JW, Johnson JA. Coordinate regulation of NAD(P)H:quinone oxidoreductase and glutathione-S-transferases in primary cultures of rat neurons and glia: role of the antioxidant/electrophile responsive element. *Glia.* 1999; 25:131-142.
- Li N, Ragheb K, Lawler G, Sturgis J, Rajwa B, Melendez JA, Robinson JP. Mitochondrial complex I inhibitor rotenone induces apoptosis through enhancing mitochondrial reactive oxygen species production. *J Biol Chem.* 2003; 278:8516-8525.
- Park S, Kim, Y., Lee, J, Seo, H., Nam, S. J., Jo, D. G., Hyun, D. H. 4-Hydroxycinnamic acid attenuates neuronal cell death by inducing expression of plasma membrane redox enzymes and improving mitochondrial functions. *Food Science and Human Wellness.* 2023; 12:1287-1299.
- Koh JH, Kim JY. Role of PGC-1alpha in the mitochondrial NAD(+) pool in metabolic diseases. *Int J Mol Sci.* 2021; 22:4558.
- Hyun DH, Kim J, Moon C, Lim CJ, de Cabo R, Mattson MP. The plasma membrane redox enzyme NQO1 sustains cellular energetics and protects human neuroblastoma cells against metabolic and proteotoxic stress. *Age (Dordr).* 2012; 34:359-370.

23. Xiao W, Wang RS, Handy DE, Loscalzo J. NAD(H) and NADP(H) redox couples and cellular energy metabolism. *Antioxid Redox Signal*. 2018; 28:251-272.
24. Lapenna D. Glutathione and Glutathione-dependent Enzymes: From biochemistry to gerontology and successful aging. *Ageing Res Rev*. 2023; 92:102066.
25. Zhong O, Wang J, Tan Y, Lei X, Tang Z. Effects of NAD<sup>+</sup> precursor supplementation on glucose and lipid metabolism in humans: a meta-analysis. *Nutr Metab (Lond)*. 2022; 19:20.
26. Zamaraeva MV, Sabirov RZ, Maeno E, Ando-Akatsuka Y, Bessonova SV, Okada Y. Cells die with increased cytosolic ATP during apoptosis: a bioluminescence study with intracellular luciferase. *Cell Death Differ*. 2005; 12:1390-1397.
27. Luengo A, Li Z, Gui DY, Sullivan LB, Zagorulya M, Do BT, Ferreira R, Naamati A, Ali A, Lewis CA, Thomas CJ, Spranger S, Matheson NJ, Vander Heiden MG. Increased demand for NAD(+) relative to ATP drives aerobic glycolysis. *Mol Cell*. 2021; 81:691-707.
28. Su LJ, Zhang JH, Gomez H, Murugan R, Hong X, Xu D, Jiang F, Peng ZY. Reactive oxygen species-induced lipid peroxidation in apoptosis, autophagy, and ferroptosis. *Oxid Med Cell Longev*. 2019; 2019:5080843.
29. Lee J, You JH, Shin D, Roh JL. Inhibition of glutaredoxin 5 predisposes cisplatin-resistant head and neck cancer cells to ferroptosis. *Theranostics*. 2020; 10:7775-7786.
30. Lee J, You JH, Roh JL. Poly(rC)-binding protein 1 represses ferritinophagy-mediated ferroptosis in head and neck cancer. *Redox Biol*. 2022; 51:102276.
31. Ivan M, Kondo K, Yang H, Kim W, Valiando J, Ohh M, Salic A, Asara JM, Lane WS, Kaelin WG, Jr. HIF1 $\alpha$  targeted for VHL-mediated destruction by proline hydroxylation: implications for O<sub>2</sub> sensing. *Science*. 2001; 292:464-468.
32. Lee J, Roh JL. Targeting iron-sulfur clusters in cancer: opportunities and challenges for ferroptosis-based therapy. *Cancers (Basel)*. 2023; 15:2694.
33. Oh ET, Kim HG, Kim CH, Lee J, Kim C, Lee JS, Cho Y, Park HJ. NQO1 regulates cell cycle progression at the G2/M phase. *Theranostics*. 2023; 13:873-895.
34. Doll S, Proneth B, Tyurina YY, *et al*. ACSL4 dictates ferroptosis sensitivity by shaping cellular lipid composition. *Nat Chem Biol*. 2017; 13:91-98.
35. Antonny B, Vanni S, Shindou H, Ferreira T. From zero to six double bonds: phospholipid 20unsaturation and organelle function. *Trends Cell Biol*. 2015; 25:427-436.
36. Brown MD, Hart C, Gazi E, Gardner P, Lockyer N, Clarke N. Influence of omega-6 PUFA arachidonic acid and bone marrow adipocytes on metastatic spread from prostate cancer. *Br J Cancer*. 2010; 102:403-413.
37. Rouault TA. Iron metabolism in the CNS: implications for neurodegenerative diseases. *Nat Rev Neurosci*. 2013; 14:551-564.
38. Zhan S, Lu L, Pan SS, Wei XQ, Miao RR, Liu XH, Xue M, Lin XK, Xu HL. Targeting NQO1/GPX4-mediated ferroptosis by plumbagin suppresses *in vitro* and *in vivo* glioma growth. *Br J Cancer*. 2022; 127:364-376.
39. Fournier M, Monin A, Ferrari C, Baumann PS, Conus P, Do K. Implication of the glutamate-cystine antiporter xCT in schizophrenia cases linked to impaired GSH synthesis. *NPJ Schizophr*. 2017; 3:31.
40. Cerutti R, Pirinen E, Lamperti C, Marchet S, Sauve AA, Li W, Leoni V, Schon EA, Dantzer F, Auwerx J, Viscomi C, Zeviani M. NAD(+)-dependent activation of Sirt1 corrects the phenotype in a mouse model of mitochondrial disease. *Cell Metab*. 2014; 19:1042-1049.
41. Kussmaul L, Hirst J. The mechanism of superoxide production by NADH:ubiquinone oxidoreductase (complex I) from bovine heart mitochondria. *Proc Natl Acad Sci U S A*. 2006; 103:7607-7612.
42. Bai P, Canto C. The role of PARP-1 and PARP-2 enzymes in metabolic regulation and disease. *Cell Metab*. 2012; 16:290-295.
43. Higgins CB, Mayer AL, Zhang Y, Franczyk M, Ballentine S, Yoshino J, DeBosch BJ. SIRT1 selectively exerts the metabolic protective effects of hepatocyte nicotinamide phosphoribosyltransferase. *Nat Commun*. 2022; 13:1074.
44. Price NL, Gomes AP, Ling AJ, *et al*. SIRT1 is required for AMPK activation and the beneficial effects of resveratrol on mitochondrial function. *Cell Metab*. 2012; 15:675-690.
45. Zhu Y, Zhang JL, Yan XJ, Ji Y, Wang FF. Exploring a new mechanism between lactate and VSMC calcification: PARP1/POLG/UCP2 signaling pathway and imbalance of mitochondrial homeostasis. *Cell Death Dis*. 2023; 14:598.
46. Almeida A, Almeida J, Bolanos JP, Moncada S. Different responses of astrocytes and neurons to nitric oxide: the role of glycolytically generated ATP in astrocyte protection. *Proc Natl Acad Sci U S A*. 2001; 98:15294-15299.
47. Herrero-Mendez A, Almeida A, Fernandez E, Maestre C, Moncada S, Bolanos JP. The bioenergetic and antioxidant status of neurons is controlled by continuous degradation of a key glycolytic enzyme by APC/C-Cdh1. *Nat Cell Biol*. 2009; 11:747-752.

Received January 29, 2024; Revised March 29, 2024; Accepted April 7, 2024.

#Present address: Logsynk, Seoul, Korea.

\*Address correspondence to:

Dong-Hoon Hyun, Department of Life Science, Ewha Womans University, Seoul 03760, South Korea.

E-mail: hyundh@ewha.ac.kr

Released online in J-STAGE as advance publication April 10, 2024.